Response Estimation Method of Buildings due to Waterborne Debris Impact Loads

T. Asai

Department of Architecture, The University of Tokyo, Tokyo, Japan.

K. Matsukawa, H. Choi & Y. Nakano

Institute of Industrial Science, The University of Tokyo, Tokyo, Japan.

ABSTRACT: The past damage observations after the tsunami disasters indicate that the waterborne debris can cause serious damage to buildings. The building response due to the debris impact loads, however, has not been sufficiently discussed. Therefore, in this paper, a rectangular pulse is defined as an impact load due to ships and shipping containers, and the defined load is applied to a particular floor of a six-story reinforced concrete building model. The elastic responses of the building due to the defined loads are then computed by modal analyses. It is found that the time when the story drift reaches its maximum value, which is either before or after the termination of the loading, depends on the impact duration. Two simplified approaches are therefore proposed considering the impact duration to roughly estimate the maximum story drifts. As a result, the maximum story drifts estimated by the proposed approaches are found in a good agreement with those computed by modal analyses.

1 INTRODUCTION

After the 2011 Great East Japan Earthquake, tsunami loads were evaluated based on the damage observations (Asai et al. 2012), and a structural design code for tsunami evacuation buildings was established (MLIT 2011). However, impact loads due to waterborne debris were not considered quantitatively in the code. Waterborne debris were reported to cause damage to buildings (PARI 2011), and design methods against the debris impact loads are therefore currently in urgent need for designing safe tsunami evacuation buildings. In the previous researches, impact loads due to wood poles, ships and shipping containers have been examined through experiments (Matsutomi 1999, Mizutani et al. 2007 and Aghl et al. 2014), but the building responses were not focused in the discussions.

In this paper, the impact load is firstly defined to understand the building responses due to the debris impact loads. Secondly, the responses due to the defined loads are computed by applying modal analyses to a particular reinforced concrete building. Finally, simplified approaches are proposed to estimate the responses due to the debris impact loads.

2 DEFINITION OF IMPACT LOADS

In this paper, impact loads due to ships and shipping containers are considered. Because the building response is significantly affected by the impact duration (Umemura et al. 1964), impact loads are defined focusing on its durations.

2.1 Impact loads due to ships

After the ship collision, ships were often found collapsed only at their bows whereas other parts had minor damage (Kiyomiya et al. 1996). Impact forces due to ships are, therefore, defined based on the collision strength of its bow. The strength P_{cr} (tf) was formulated considering the buckling strength of ship-hull plate, and it was examined by static loading tests (Nagasawa et al. 1977). The strength P_{cr} was then expressed as a function of gross tonnage of a ship T_G (G.T.) as Eq. (1), considering the statistical relationship between T_G and the thickness of the hull plate (Shoji et al. 1999).

$$P_{cr} = 1.17{T_G}^{1/3}\left(0.82{T_G}^{1/6} + 1\right)^3 \quad (1)$$

In this paper, an impact load due to a ship is defined as a rectangular pulse with its constant force F (kN) equal to P_{cr}. Then the impact duration τ (s) is defined as Eq. (3) assuming a completely inelastic collision (i.e., the coefficient of restitution e is 0, and the impulse of the load is mv).

$$F = P_{cr}\, g \tag{2}$$

$$\tau = mv/F \tag{3}$$

where m (t) and v (m/s) are the mass and velocity of a debris, respectively; g (m/s^2) is the gravity acceleration. For example, an impact force F and an impact duration τ of a 200 G.T. ship, assuming its displacement tonnage (i.e., its weight) 300 tons, at a speed of 3 m/s are calculated about 1800 kN and 0.5 s, respectively.

2.2 **Impact loads due to shipping containers**

A time history of an impact load due to a shipping container was proposed theoretically considering the stress wave propagation, and it was examined by full-scale in-air experiments (Aghl et al. 2014). In that study, an impact load was defined as a rectangular pulse, with its force F and impact duration τ were expressed by Eqs. (4) and (5), respectively. A completely elastic collision was assumed here (i.e., the coefficient of restitution e is 1.0, and the impulse of the load is $2mv$).

$$F = \sqrt{km}v \tag{4}$$

$$\tau = 2mv/F \tag{5}$$

where k (kN/m) is the effective stiffness of a container. The effect of water was concluded negligible based on the in-water tests. Referring to the study, impact loads defined by Eqs. (4) and (5) are employed in this paper. An impact force F and an impact duration τ due to a 20 ft standard container colliding at a speed of 3 m/s are, for example, calculated about 1300 kN and 0.01 s, respectively.

2.3 **Impact loads employed in this study**

Considering the discussions mentioned above, the impact loads are defined as a rectangular pulse as shown in Fig. 1, with its impact duration τ varying from 0.004 s to 0.5 s to include the impact duration due to ships and shipping containers as described earlier. Then the building response characteristics due to the defined loads are analysed.

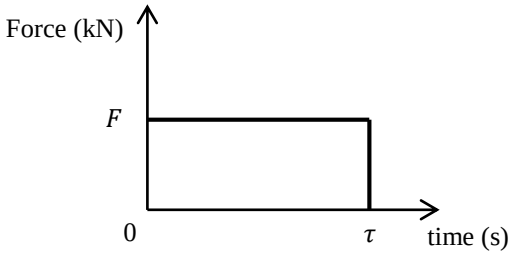

Fig. 1 Defined time history of impact loads

3 **ELASTIC RESPONSE CHARACTERISTICS DUE TO IMPACT LOADS**

3.1 **Response computed by modal analysis**

Modal analyses are firstly made to compute the responses of a multi-mass shear system exposed to the defined impact loads. The responses before the loading is terminated are firstly obtained, then based on the responses, those after the loading is terminated are derived. From the equation of motion expressed by Eq. (6), a displacement response vector $\{y\}$ is obtained as Eq. (7) when the i-th floor is loaded by the constant force F (kN). Here, the damping is considered proportional to the stiffness.

$$[M]\{\ddot{y}\} + [C]\{\dot{y}\} + [K]\{y\} = \{f(t)\} \tag{6}$$

$$\{y\} = \sum_{s=1}^{N} \{ {}_s u\}\, {}_s u_i \frac{F}{{}_s K} \left\{ 1 - e^{-\,{}_s h\, {}_s \omega t} \left(\cos\, {}_s \omega' t + {}_s h \left({}_s \omega / {}_s \omega' \right) \sin\, {}_s \omega' t \right) \right\} \tag{7}$$

$$ {}_s\omega' = \sqrt{1 - {}_sh^2}\ {}_s\omega $$

where $[M]$ (t), $[C]$ and $[K]$ (kN/m) are mass, damping and stiffness matrixes, respectively; $\{y\}$ (m) and $\{f(t)\}$ (kN) are the displacement and force vector; $\{ {}_su\}$ is the s-th order mode vector normalized so that $\{ {}_su\}^T\{ {}_su\} = 1$; ${}_sK$ (kN/m), ${}_sh$ and ${}_s\omega$ (1/s) are the s-th order generalized stiffness, damping factor and angular frequency, respectively; t (s) is the time. Given damping factor ${}_sh$ is zero, Eq. (7) leads to Eq. (8).

$$ \left\{y|_{\ {}_sh=0}\right\} = \sum_{s=1}^{N}\{ {}_su\}\ {}_su_i \frac{F}{{}_sK}\left(1 - \cos\ {}_s\omega t\right) \tag{8} $$

The story drift of the j-th story is then obtained as Eq. (9).

$$ y_j - y_{j-1}|_{\ {}_sh=0} = \sum_{s=1}^{N}\left({}_su_j - {}_su_{j-1}\right)\ {}_su_i \frac{F}{{}_sK}\left(1 - \cos\ {}_s\omega t\right) \tag{9} $$

Here, a part of Eq. (9), $\sum_{s=1}^{N}\ {}_su_i\ {}_su_j/\ {}_sK$, corresponds to an element α_{ij} of flexibility matrix $[\alpha]$ (m/kN) through Eq. (10).

$$ \left[\sum_{s=1}^{N}\frac{{}_su_i\ {}_su_j}{{}_sK}\right] = [U]\left[\ {}_sK\right]^{-1}[U]^T = [U]([U]^T[K][U])^{-1}[U]^T = [K]^{-1} = [\alpha] \tag{10} $$

An element α_{ij} of $[\alpha]$ is the displacement of the j-th floor per unit force acted on the i-th floor. The story drift of the j-th floor $\alpha_{ij} - \alpha_{ij-1}$ below the i-th loaded floor (i.e., $i \geq j$) is therefore obtained as $1/K_j$ (K_j (kN/m) is the story stiffness of the j-th story), and the story drift above the loaded floor (i.e., $i < j$) is zero because no shear force acts above the i-th floor. Considering the discussion mentioned above, Eq. (11) is obtained.

$$ \begin{aligned} \sum_{s=1}^{N}\frac{\left({}_su_j - {}_su_{j-1}\right)\ {}_su_i}{{}_sK} = \alpha_{ij} - \alpha_{ij-1} &= \frac{1}{K_j} \quad (i \geq j) \\ &= 0 \quad (i < j) \end{aligned} \tag{11} $$

The story drift before the loading is terminated (i.e., $t \leq \tau$) is then obtained from Eqs. (9) and (11).

$$ \begin{aligned} y_j - y_{j-1}|_{\ {}_sh=0} &= \frac{F}{K_j} - \sum_{s=1}^{N}\left({}_su_j - {}_su_{j-1}\right)\ {}_su_i \frac{F}{{}_sK}\cos\ {}_s\omega t \quad (i \geq j) \qquad (t \leq \tau) \\ &= \quad -\sum_{s=1}^{N}\left({}_su_j - {}_su_{j-1}\right)\ {}_su_i \frac{F}{{}_sK}\cos\ {}_s\omega t \quad (i < j) \qquad (t \leq \tau) \end{aligned} \tag{12} $$

The displacement vector $\{y'\}$ (m) after the loading is terminated (i.e., $t > \tau$) is obtained through combining the response by Eq. (7) and the response due to the force $(-F)$ imposed in the opposite direction.

$$ \{y'(t)\} = \{y(t)\} - \{y(t-\tau)\} \qquad (t > \tau) \tag{13} $$

In the same way, given damping factor ${}_sh$ is zero, the story drift of the j- th story after the loading is terminated (i.e., $t > \tau$) is obtained as Eq. (14) from Eq. (12).

$$ y'_j - y'_{j-1}|_{\ {}_sh=0} = -\sum_{s=1}^{N}\left({}_su_j - {}_su_{j-1}\right)\ {}_su_i \frac{F}{{}_sK}\left(\cos\ {}_s\omega t - \cos\ {}_s\omega(t-\tau)\right) \quad (t > \tau) \tag{14} $$

When τ approaches zero, Eq. (15) is derived from Eq. (14) considering $F = I/\tau$ (I (kNs) is the momentum of the impact load).

$$ y'_j - y'_{j-1}|_{\ {}_sh=0,\tau\to 0} = \sum_{s=1}^{N}\left({}_su_j - {}_su_{j-1}\right)\ {}_su_i \frac{{}_s\omega I}{{}_sK}\sin\ {}_s\omega t \qquad (t > \tau) \tag{15} $$

Eventually, Eq. (15) corresponds to the unit impulse response with no damping.

3.2 **Elastic response characteristics due to impact loads**

Based on the responses obtained above, the building response characteristics due to the impact loads are analysed. A six story reinforced concrete building designed to an expected tsunami wave load (NILIM 2012) is substituted for MDOF model with elastic stiffness and an impact load is applied to a particular

floor. The floor and elevation plan of the building are shown in Fig. 2. The mass of the each floor M is 893 t. The building is boxed wall-building and its natural period in the direction parallel to the load is 0.22 s. A participation vector of the model is shown in Fig. 3. The model is exposed to the impact load, with its momentum Mv defined as 893 tm/s, and the response characteristics are parametrically analysed to different impact durations.

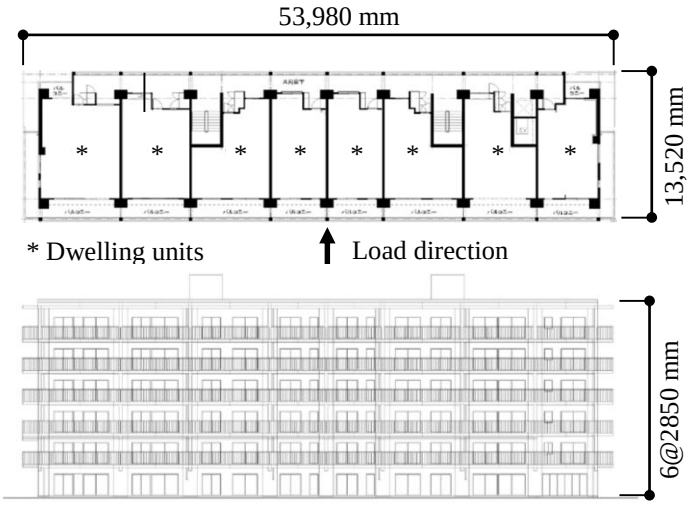

Fig. 2 Floor and elevation plans of example building

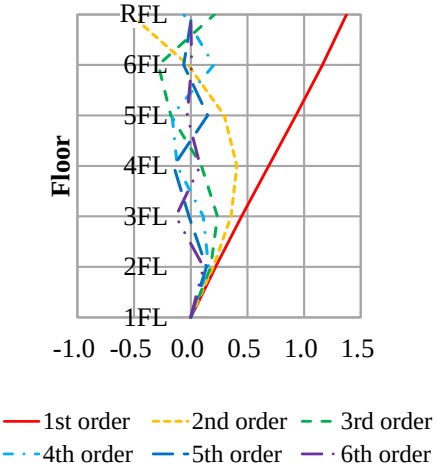

Fig. 3 Participation vectors of model

Firstly, the maximum story drifts due to the impact loads are computed by Eqs. (7) and (13), as shown in Figs. 4 and 5. Fig. 4 shows the maximum story drifts spectra when 2 FL, 4 FL, or 6 FL is loaded with the impact duration τ varying from 0.004 s to 0.5 s. Fig. 5 shows the maximum story drifts along the building's height when one single floor is loaded with the impact duration τ of 0.01 s, 0.2 s and 0.5 s. Major findings from Figs. 4 and 5 are as follows:

1. Fig. 4 shows that the maximum story drift increases as the impact duration τ decreases.
2. As shown in Fig. 5, when the impact duration τ is 0.2 s or 0.5 s, the maximum story drifts have large differences in floor levels below and above the loaded floor; the maximum story drifts below the loaded floor levels are larger than the others. Their variations are small in floor levels below

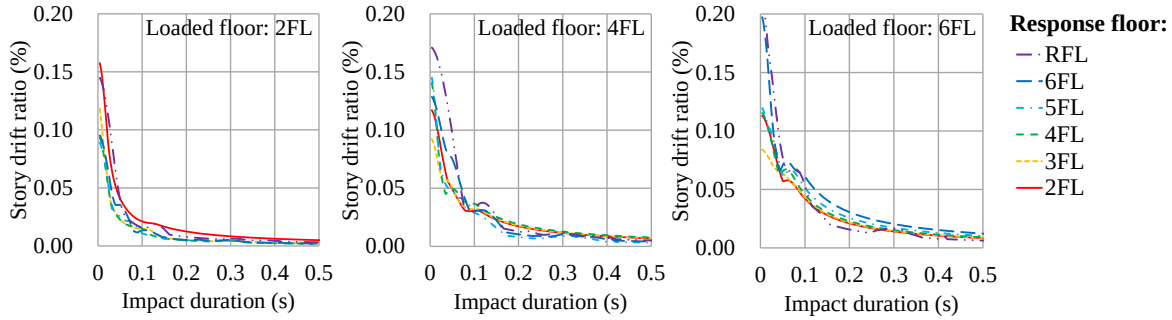

Fig. 4 Maximum story drifts spectra ($_1h$= 0.02)

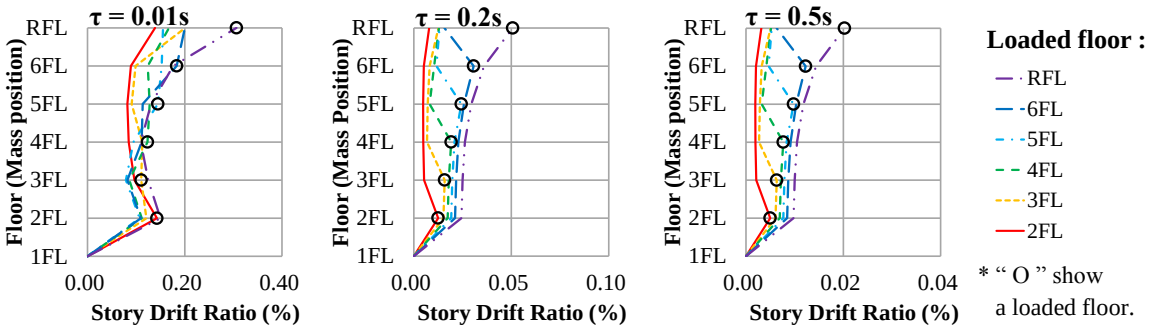

Fig. 5 Maximum story drifts along building's height ($_1h$= 0.02)

and above the loaded floor levels, respectively. In case of τ = 0.01 s, however, the loaded floor level is not a significant point to create a distinctive difference in response unlike the case of τ = 0.2 s or 0.5 s.

Secondly, the time histories of the story drifts before and after the termination of the loading are computed by Eqs. (12) and (14), respectively, and they are shown in Fig. 6. Note that the damping factor ${}_sh$ is assumed zero herein, as described in the previous section. Fig. 6 shows the time histories of the second and sixth story drifts, together with their each modal responses and F/K_j in Eqs. (12) and (14), when the second or sixth floor is loaded with impact duration τ equal to 0.01 s and 0.2 s. Major findings from Fig. 6 are as follows:

1. The responses of higher-order modes are not always negligibly small compared to the lower-order modes, unlike general building responses to an earthquake.
2. When the impact duration τ is 0.01 s, which is much shorter than the natural period of the building ${}_1T$, the maximum story drifts ($\star$ in Fig.) appears after the termination of the loading (∇ in Fig.).
3. When the impact duration τ is 0.2 s, which is almost equal to the natural period of the building ${}_1T$, the maximum story drifts ($\star$ in Fig.) appears before the termination of the loading (∇ in Fig.).

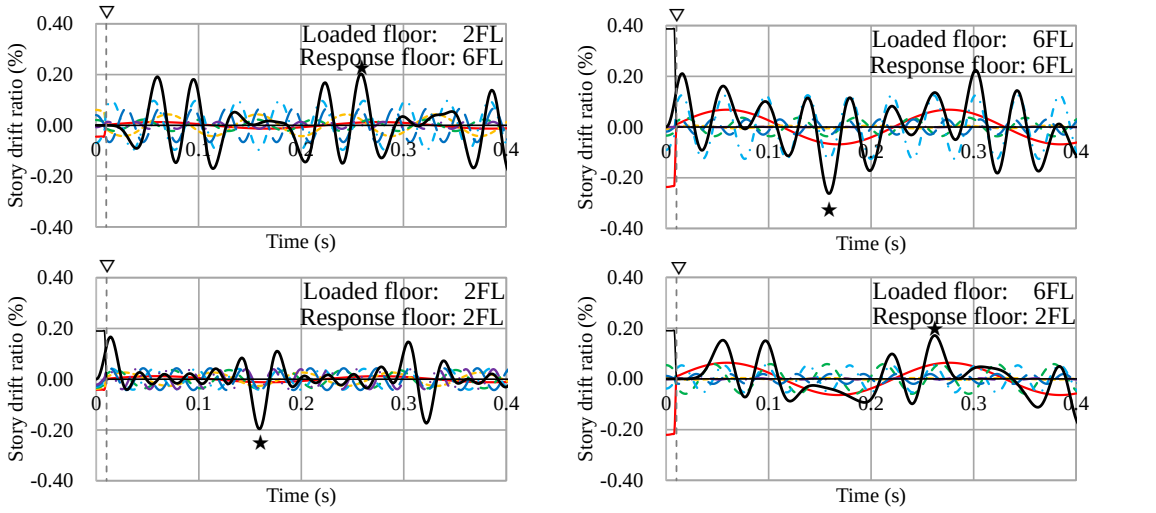

Impact duration τ = 0.01s

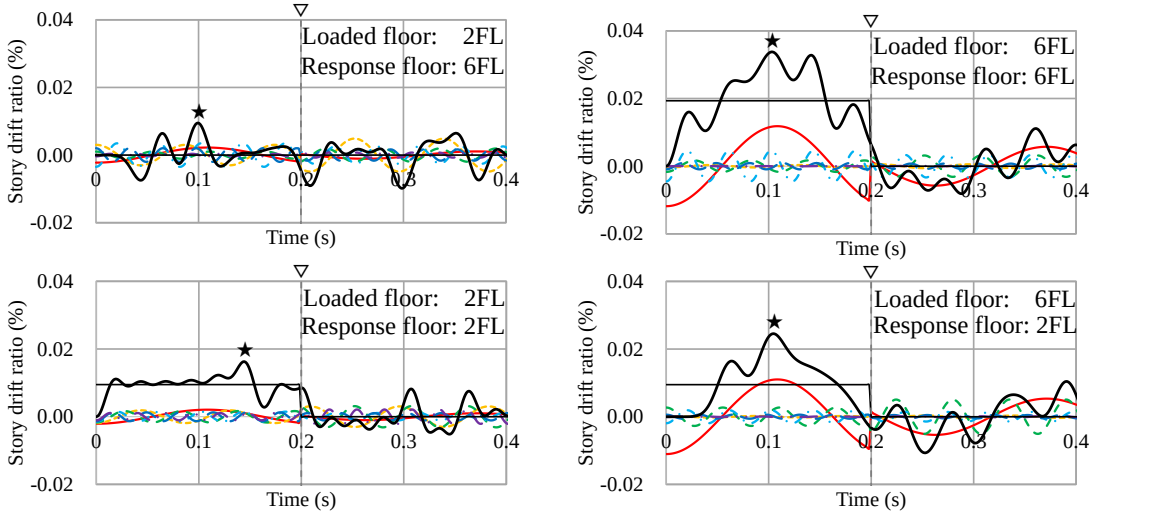

Impact duration τ = 0.2s

Fig. 6 Time histories of story drifts (${}_1h$= 0)

As described in the above findings, it is found that the time when the story drift reaches its maximum value, which is either before or after the termination of the loading, depends on the impact duration τ. The story drifts before and after the termination of the loading are computed by different equations, Eq. (12) and Eq. (14) (or Eq. (15) when τ approaches zero), respectively, as mentioned in the previous section.

4 RESPONSE ESTIMATION BY SIMPLIFIED PROCEDURE

The building responses due to the debris impact loads are obtained and their characteristic are investigated in the previous chapter. Because the maximum story drifts are generally considered as criteria for the practical design, a simple method to estimate them are discussed here. As described in the previous chapter, the maximum story drifts are obtained by the two different equations depending on the impact duration τ. Those equations are therefore simplified considering the impact duration to roughly estimate the maximum story drifts. SRSS (Square Root of Sum of Squares) modal combination method is applied for the simplified procedure.

4.1 In case of shorter impact duration

When the impact duration τ is much shorter than the natural period of the building ${}_1T$ (0.22 s), the story drifts at their maximum value are computed by Eq. (14) (or Eq. (15) when τ approaches zero) as described in the previous chapter. Here, considering the extreme condition that τ approaches zero, Eq. (15) (i.e., the unit impulse response) instead of Eq. (14) is simplified by SRSS modal combination method, and Eq. (16) is obtained to estimate the maximum story drift δ_{j1}.

$$\delta_{j1} = \sqrt{\sum_{s=1}^{N} \left| \left({}_s u_j - {}_s u_{j-1} \right) {}_s u_i \frac{{}_s \omega I}{{}_s K} \right|^2} \tag{16}$$

The maximum story drifts estimated by Eq. (16) and those computed by modal analyses (i.e., computed by Eqs. (7) and (13)) are then compared in Fig. 7. As shown in the figure, the estimated values obtained from Eq. (16) are about 0.6 to 1.5 times of the story drifts computed by modal analysis when τ approaches zero. As the impact duration τ increases, however, the differences between the result of the estimation equations and that of modal analyses become larger. The other approach is therefore proposed considering the longer impact duration.

4.2 In case of longer impact duration

When the impact duration τ is longer than the natural period of the building ${}_1T$ (0.22 s), the story drifts at their maximum value are computed by Eq. (12) as described in the previous chapter. Eq. (12) is then simplified by SRSS modal combination method, and Eq. (17) is obtained to estimate the maximum story drift δ_{j2}.

$$\begin{aligned} \delta_{j2} &= \frac{F}{K_j} + \sqrt{\sum_{s=1}^{N} \left| \left({}_s u_j - {}_s u_{j-1} \right) {}_s u_i \frac{F}{{}_s K} \right|^2} \quad (i \geq j) \\ &= \sqrt{\sum_{s=1}^{N} \left| \left({}_s u_j - {}_s u_{j-1} \right) {}_s u_i \frac{F}{{}_s K} \right|^2} \quad (i < j) \end{aligned} \tag{17}$$

Figure 7 shows that the maximum story drifts estimated by Eq. (17) are found in a good agreement with the results of modal analyses except when the impact duration τ approaches zero.

4.3 Accuracy of response estimation method

Considering the discussions in the previous sections, the minimum of the two values estimated by Eqs. (16) and (17) (i.e., Eq. (18)) is assumed to be in a good agreement with the results of modal analyses.

$$\delta_j = min(\delta_{j1}, \delta_{j2}) \tag{18}$$

To evaluate the accuracy of the estimation Eq. (18), the ratios of the maximum story drifts estimated by

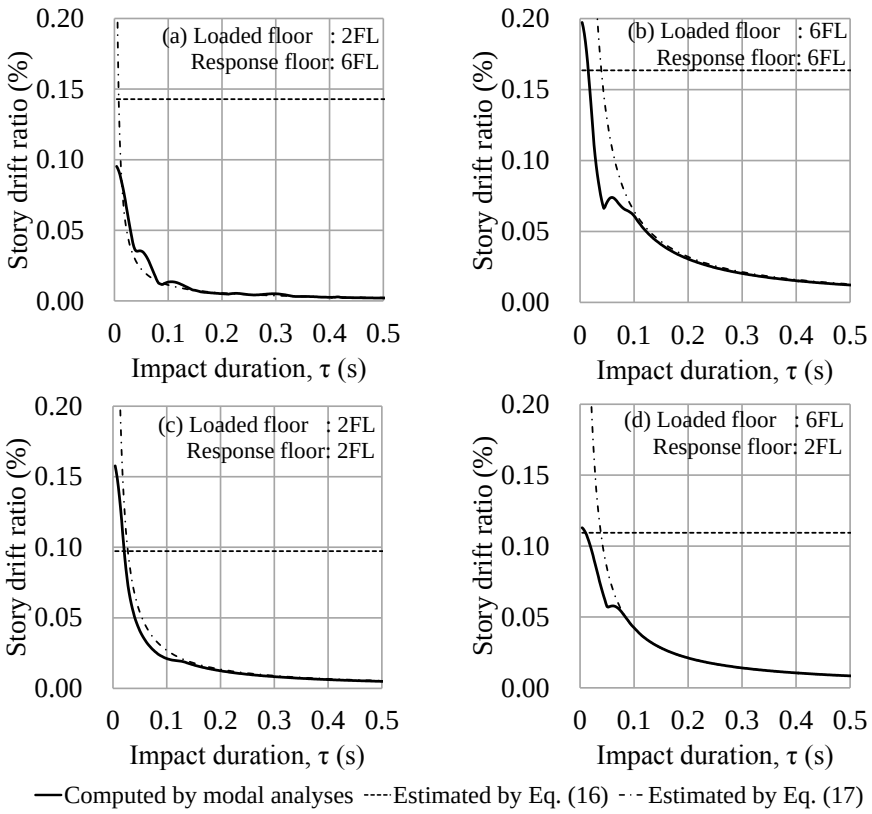

Fig. 7 Maximum story drifts computed by modal analyses and estimated by Eqs. (16) and (17)

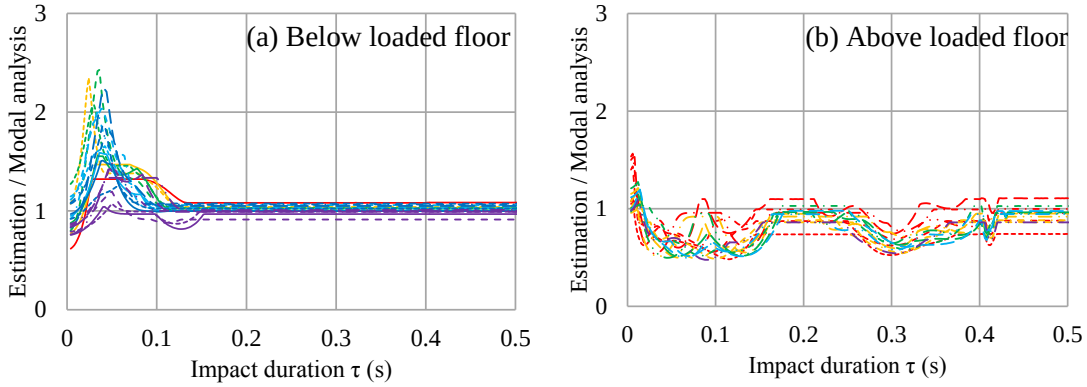

Fig. 8 Ratio of estimated maximum story drifts to that computed by modal analyses

Eq. (18) to those computed by modal analyses are shown in Fig. 8. The results below and above the loaded floor are shown in Fig. 8(a) and (b), respectively. As shown in Fig. 8(a), the estimated maximum story drifts below the loaded floor are found in a good agreement with the results of modal analyses when the impact duration τ is longer than 0.15 s. When τ is shorter than 0.15 s, however, the maximum story drifts are generally overestimated, and they are about 1.0 to 2.5 times of modal analysis results. On the other hand, the estimated maximum story drifts above the loaded floor vary from 0.5 to 1.0 times of modal analyses as shown in Fig. 8(b). It should be noted that the results above the loaded floor are not conservatively estimated.

5 CONCLUSIONS

To propose an estimation method of a building response due to the debris impact loads, an impact load

is defined and applied to a particular reinforced concrete building model. The building responses are then computed by modal analyses, and simplified approaches are proposed to roughly estimate the maximum story drifts of the building. The major findings can be summarized as follows:

1. Impact loads due to ships and shipping containers are defined as a rectangular pulse, referring to the studies to evaluate collision strength of a ship's bow and those to obtain a time history of an impact load due to a shipping container.
2. Based on the responses computed by modal analyses, it is found that the time when the story drift reaches its maximum value, which is either before or after the termination of the loading, depends on the impact duration. Two simplified approaches are therefore proposed considering the impact duration, and Eqs. (16), (17) and (18) are obtained to estimate the maximum story drifts.
3. The maximum story drifts below the loaded floor estimated by Eqs. (16), (17) and (18) are found in a good agreement with the results of modal analyses when the impact duration τ is longer than about 0.15s. When τ is shorter than about 0.15s, however, the maximum story drifts are generally overestimated. The estimated maximum story drifts above the loaded floor vary from 0.5 to 1.0 times of modal analyses.

The validation and practical application of the method proposed herein will be discussed elsewhere.

ACKNOWLEDGEMENT

This work was partially supported by JSPS KAKENHI Grant Number 24246093 (PI: Yoshiaki Nakano).

REFERENCES:

Aghl, P.P., Naito, C.J., Riggs, H.R. 2014. Full-Scale Experimental Study of Impact Demands Resulting from High Mass, Low Velocity Debris, *Journal of Structural Engineering,* 140 (5) 04014006 Virginia: ASCE

Asai, T., Nakano, Y., Tateno, T., Fukuyama, H., Fujima, K., Sugano, T., Haga, Y. and Okada, T. 2012. Tsunami Load Evaluation Based on Damage Observation after the 2011 Great East Japan Earthquake, *International symposium on engineering lessons learned from the giant earthquake, 54, Tokyo, March 2012.*

Kiyomiya, O., Miyagi, T., Ishikawa, M. and Kadokura, H. 1996. Evaluation of Collision Analysis of Ship to Pile Type Fender, *Journal of Japan Society of Civil Engineers,* No. 540 (6-31) 49-57 Tokyo: JSCE (in Japanese)

Matsutomi, H. 1999. A Practical Formula for Estimating Impulsive Force due to Driftwoods and Variation Features of the Impulsive Force, *Journal of Japan Society of Civil Engineers,* No. 621 (2-47) 111-127 Tokyo: JSCE (in Japanese)

Mizutani, N., Usami, A. and Koike, T. 2007. Experimental Study on Behaviour of Drifting Boats due to Tsunami and Their Collision Forces, *Annual Journal of Civil Engineering in the Ocean,* No. 23 63-68 Tokyo: JSCE (in Japanese)

MLIT/Ministry of Land, Infrastructure, Transport and Tourism, Japan. 2011. *Notification 1318* Tokyo: MLIT (in Japanese)

Nagasawa, H., Arita, K., Tani, M. and Oka, S. 1977. A Study on the Collapse of Ship Structure in Collision with Bridge Piers, *Journal of the Japan Society of Naval Architects and Ocean Engineers,* 142 323-332 Tokyo: SNAJ (in Japanese)

NILIM/National Institute for Land and Infrastructure Management, Ministry of Land, Infrastructure, Transport and Tourism, Japan. 2012. Practical Guide on Requirement for Structural Design of Tsunami Evacuation Buildings, *Technical Note of National Institute for Land and Infrastructure Management,* No.673 Tsukuba: NILIM (in Japanese) http://www.nilim.go.jp/lab/bcg/siryou/tnn/tnn0673pdf/ks0673.pdf

PARI/Port and Airport Research Institute, Japan. 2011. Urgent Survey for 2011 Great East Japan Earthquake and Tsunami Disaster in Ports and Coasts, *Technical Note of the Port and Airport Research Institute,* No.1231 Yokosuka: PARI (in Japanese)

Shoji, K. and Takabayashi, T. 1999. Effect of Ship Dimensions on Calculation Formula for Bow Collision Strength, *Journal of Japan Institute of Navigation,* 101 201-209 Tokyo: JIN (in Japanese)

Umemura, H. and Matsushima, Y. 1964. Response Spectra for Linear Single-degree-of freedom Systems to Various Impulse, *Journal of Structural and Construction Engineering,* 103 109 Tokyo: AIJ (in Japanese)